Hyperspectral Cytometry at the Single-Cell Level Using a 32-Channel Photodetector

Gérald Grégori,[1,2] Valery Patsekin,[1,3] Bartek Rajwa,[1,3] James Jones,[4] Kathy Ragheb,[1,3] Cheryl Holdman,[1,3] J. Paul Robinson[1,3,4]*

[1]Department of Basic Medical Sciences, School of Veterinary Medicine, Purdue University, West Lafayette, Indiana 47907

[2]Université de la Méditerranée, CNRS, Laboratoire de Microbiologie, Géochimie et Ecologie Marines, Marseille, 13288, France

[3]Bindley Bioscience Center, Purdue Univeristy, West Lafayette, Indiana 47907

[4]Weldon School of Biomedical Engineering, Purdue University, West Lafayette, Indiana 47907

*Correspondence to: J. Paul Robinson, Purdue University Cytometry Laboratories, Bindley Bioscience Center, 1203 West State Street, West Lafayette, IN 47907-2057, USA

Email: jpr@cyto.purdue.edu

- **Abstract**

Despite recent progress in cell-analysis technology, rapid classification of cells remains a very difficult task. Among the techniques available, flow cytometry (FCM) is considered especially powerful, because it is able to perform multiparametric analyses of single biological particles at a high flow rate–up to several thousand particles per second. Moreover, FCM is nondestructive, and flow cytometric analysis can be performed on live cells. The current limit for simultaneously detectable fluorescence signals in FCM is around 8–15 depending upon the instrument. Obtaining multiparametric measurements is a very complex task, and the necessity for fluorescence spectral overlap compensation creates a number of additional difficulties to solve. Further, to obtain well-separated single spectral bands a very complex set of optical filters is required. This study describes the key components and principles involved in building a next-generation flow cytometer based on a 32-channel PMT array detector, a phase-volume holographic grating, and a fast electronic board. The system is capable of full-spectral data collection and spectral analysis at the single-cell level. As demonstrated using fluorescent microspheres and lymphocytes labeled with a cocktail of antibodies (CD45/FITC, CD4/PE, CD8/ECD, and CD3/Cy5), the presented technology is able to simultaneously collect 32 narrow bands of fluorescence from single particles flowing across the laser beam in <5 μs. These 32 discrete values provide a proxy of the full fluorescence emission spectrum for each single particle (cell). Advanced statistical analysis has then been performed to separate the various clusters of lymphocytes. The average spectrum computed for each cluster has been used to characterize the corresponding combination of antibodies, and thus identify the various lymphocytes subsets. The powerful data-collection capabilities of this flow cytometer open up significant opportunities for advanced analytical approaches, including spectral unmixing and unsupervised or supervised classification. © 2011 International Society for Advancement of Cytometry

- **Key terms**

hyperspectral cytometry; flow cytometry; next-generation instruments

FLOW cytometry (FCM) is a very powerful cell-analysis technique, applied in various fields of life science ranging from basic cell biology to genetics, immunology, molecular biology, microbiology, plant cell biology, and environmental science (1). FCM uses optical properties of biological particles and makes analysis possible at the single-cell level. Forward-angle light scatter (size-related) and side-angle light scatter (shape- and structure-related) as well as various fluorescence emissions are collected following illumination/excitation (usually by one or several lasers). The data are collected, digitized, and stored on a computer where they are further processed to discriminate populations of particles (cells) with similar characteristics.

Detection systems used in current commercial instruments are almost all based on a simple concept whereby the fluorescence signal travels down an optical pathway through a set of dichroic filters, each of which splits the signal into different wavelength ranges. Fluorescence emission passes through bandpass filters of a desired wavelength or another dichroic filter to be eventually recorded by a photodetector.

International Society for Advancement of Cytometry

The resultant electronic signal is then digitized and a value is finally stored in computer memory. The photodetectors employed are typically photodiodes for the brightest signals, such as forward- and side-angle scatter, and photomultiplier tubes (PMTs) for fluorescence emission, because of the need for significant signal amplification.

Existing systems are usually quite efficient at collecting fluorescence emission and converting it quantitatively into values that can be related to biological phenomena of interest. Over the past three decades, FCM technology has developed from single-color systems to two-, three-, and four-color ones, and more recently, the use of 17 simultaneous colors has been reported (2). However, commercial systems for the most part focus on more manageable numbers of simultaneously collected variables (spectral bands), typically 5–7.

A similar tendency to increase the number of colors exists in the imaging FCM. The ImageStream system from Amnis (Seattle, WA) is a high-throughput imaging flow cytometer that combines the morphological capabilities of multiple forms of microscopy with the sample handling and quantitative power of FCM (3). Although the basic version of the instrument collects four fluorescence bands (images), the very last version offers up to 12 channels of detection with the help of an optional second camera and associated optics.

Performing measurements that require discrimination of so many fluorescence signals is cumbersome and makes interpretation of traditional unconstrained compensation difficult (4,5). However, it is also evident that with FCM hardware that allows for collection of a large number of spectral bands one may actually consider recording the full spectra of the fluorochromes used. In consequence, a significant departure from current system design and the implementation of advanced spectral unmixing and classification methods may both be possible.

The common implementation of FCM uses dichroic mirrors and bandpass filters, because it is assumed that the signal from every individual fluorochrome (hence every color) should be collected using an independent detector. It is well accepted that transmissive light loss for dichroic mirrors ranges from 5 to 15%. However, signal reflected from that same dichroic suffers a loss of about 1%. These facts are carefully considered in the design of instruments such as the LSR, CANTO, and ARIA from BD, where a very clever use of reflection angles allows a significant amount of light to be captured even with eight or more spectral bands. For the most part, however, the use of dichroic mirrors result in substantial signal losses by the time the last signal is collected. To alleviate this problem, FCM instruments are designed so that the long wavelength signals (i.e., signals of lower energy) are collected first, and at the very last the shortest available wavelength signals (in the blue region of the visible spectrum), for which energy levels are much higher. Since almost all current instruments use PMTs as detectors, there is not much variation in optical design or in dynamic range of measured signals.

Both the absorption and emission spectra of the fluorochromes used in FCM may carry valuable spectral information about tagged biological particles. The commonly used optical design of FCM instruments makes it desirable to have a series of efficient fluorochromes that have very specific and narrow excitation maxima and give reasonably narrow emission bands within the sensitivity of the detector. To achieve multiple fluorescent probe excitations and to collect multiple emissions it is necessary to employ a variety of excitation sources and a series of fluorescence probes with minimally overlapping emission spectra. This can be particularly difficult, as demonstrated in a report that showed the excitation and emission spectra of fluorochromes necessary to perform 11-color analysis (6). However, without good spectral separation, one cannot differentiate the fluorescence emissions of the fluorochromes employed. Unfortunately, because almost all organic dyes have broad emission spectra it is virtually impossible to measure signal from one fluorochrome to the complete exclusion of any other. This is the ultimate limitation of current FCM systems (4,6,7).

It was recognized very early that collecting full emission spectra from microparticles in flow would provide much more information about the specimen being analyzed than measuring just a few predefined bands. As early as 1979, Wade et al. reported recording the fluorescence spectrum of particles in a flow system (8). However, the design of the instrumentation allowed only collection of integrated spectra from many particles (not from an individual particle) and assumed homogeneity of the sample. Steen and Stokke measured averaged fluorescence spectra of rat thymocytes in 1986, using a custom-built cytometer and grating monochromator (9,10). In 1990, Buican used a Fourier-transform interferometer to obtain single-cell spectra (11). The performance of his design was severely limited by the fact that cells needed to stay in the laser beam for a relatively long time to be scanned; modern high-speed flow cytometers use a laser excitation time of ∼1–10 μs. Yet another design based on a flint-glass prism and an intensified photodiode array was proposed by Gauci et al. in 1996 (12). Again, the data rate of the instrument was too slow to be of practical use. Additionally, the efficiency of photodiodes was (and still is) below the power offered by PMT technology. In the same year (1996), Asbury et al. measured spectra of cells and chromosomes using a monochromator, changing the wavelength during the course of an instrument run (12,13). The technique allowed measurement of just a single band from any individual particle. SoftRay and a group of researchers from the Universities of Wyoming and Utah pursued another prism-based concept (14). However, there have been no subsequent reports from this program.

More recently, in 2006, Goddard et al. presented a system that uses a diffraction grating to disperse the collected fluorescence and side-scattered light and a CCD image sensor coupled to a spectrograph to collect the signals (15). The system was built around the flow cell and collection optics of a conventional flow cytometer with minimal modifications. Based on the hardware, a traditional flow rate (i.e., several thousand cells per second) could be expected. Surprisingly, according to the description in their Materials and Methods (sample concentration: 1.7×10^5 particles/ml; sample delivery: 15 μl/min) the flow-rate analysis turns out to be lower

(∼42 particles/s) to minimize coincident events during the exposure and readout intervals of the CCD array. Even though the cited work does not indicate that that is the upper limit to particle analysis rates, this is most certainly the flow rate used with that very instrument. Very likely, faster CCD readout electronics would allow higher analysis rates without coincidence. In 2008, work carried out by John Nolan's group (La Jolla Bioengineering Institute) outlined the development of a Raman spectral flow cytometer (16). Raman spectroscopy, via surface-enhanced Raman (SERS), and FCM were brought together by substituting a dispersive-optic spectrograph with multichannel detector (CCD) in place of the traditional mirrors/beam splitters, filters, and photomultipliers (PMTs) of conventional flow cytometers. Although intrinsic Raman scattering is an inefficient process that produces low signal intensities, several variants of the technique with enhanced Raman scattering signals are able to provide stronger signals, sometimes as bright as those from fluorescent probes. For instance, SERS has been considered for applications requiring sensitive detection. Metal nanoparticle—based SERS probes are being developed that exhibit bright and characteristic Raman spectra, demonstrated in several bulk- and image-based detection applications. The system is of sufficient sensitivity to detect and analyze with good spectral resolution SERS spectra from samples consisting of nanoparticle SERS tags bound to microspheres. The instrument can measure Raman spectra from particles bearing as few as ∼200 Raman probes and can make measurements with integration times as short as 100 μs. Results obtained with the instrument show that it can detect more probes in a spectral range than traditional systems can. However, the development of robust reagents is an important challenge. Indeed, unlike organic fluorophores or fluorescent proteins, which can be prepared with high purity, nanoparticle-based SERS systems tend to be relatively heterogeneous. Even though researchers have made SERS systems reproducible (17,18), the process requires special care, and engineering improved nanoparticle SERS systems remains an important objective (3,19). Regrettably, none of these interesting technologies and design ideas has had any impact on the development of widely used clinical or research-grade flow cytometers.

The goal of the reported research was to develop hardware and software prototypes for fast classification of particles in flow using a spectral extension of FCM techniques. The rationale behind the described work is the attempted reduction in the complexity of optical paths and detection systems in FCM in favor of a simple yet powerful single-detector approach that offers portability, robustness, and adaptability to automation. We developed our original prototype of a spectral FCM instrument using a first-generation 32-channel multianode PMT (20). Although the available detector offered only limited sensitivity, the system demonstrated the feasibility of spectral data collection in flow (21,22). We have expanded on our original design with a more sensitive detection system that can measure a spectral emission pattern within the normal time scale of a regular FCM instrument, which is between 1 and 10 μs per particle. The reported design uses a 32-channel PMT for full spectral detection accompanied by a traditional custom-built polychromatic

detection unit using dichroic filters. This instrument allows traditional or spectral measurements, as well as simultaneous spectral and polychromatic data collection. The performed tests show that comparable results can be obtained, and for specific applications, the spectral subsystem can perform similarly to a polychromatic subsystem, employing significantly simplified optical path and detection components.

MATERIAL AND METHODS

Spectral Subsystem

The fundamentals of the design are described in our first report of the spectral FCM system (23). Briefly, the signal coming from the interrogation volume (i.e., where particles are intercepted one by one by the laser beam) consists in a polychromatic source collected at 90° to the laser direction (Fig. 1A). The various wavelengths are then dispersed by a phase-volume holographic grating (Kaiser Optical Systems, Ann Arbor, MI) onto a photodetector, which is a Hamamatsu 7260-01 32-channel multianode PMT linear array (Fig. 1B). The PMT offers luminous sensitivity of 250 μA/lm. The typical uniformity between each anode is 1:1.7. The effective area per channel is 0.8×7 mm, with a channel pitch of 1 mm. The detailed specifications of the employed linear-array PMT are provided in the Supporting Information.

High-Speed Data Acquisition System

The crucial aspect of the reported prototype is the ability to register the entire emission spectrum (approximated by 32 channels) of a single biological particle in addition to its scatter signals within the time that the particle traverses the regular detection volume. In a normal FCM instrument data rates of 1,000–100,000 events per second are routinely obtained; this means that a particle may be available for analysis for <10 μs. Therefore, to obtain a full spectrum, high-speed electronics are necessary. The high-speed data acquisition is performed by a PhotoniQ-OEM Model 3214 board with 32 channels (Vertilon Corporation, Westford, MA). In addition, a daughter board with an additional 32 channels was added to provide 64 channels with 14 bits/channel resolution.

The integration time of the PhotoniQ-OEM Model 3214 is set by a resistor-capacitor network. We used an external trigger signal (the side-scatter signal from the Coulter Epics Elite), which added an overhead and incurred a variable synchronization delay (∼0–15 ns) before the start of integration. Generally, longer integration time events tolerate a few nanoseconds of uncertainty in their start time using the employed electronics. Under digital control, the integration time and the average delay from trigger may be controlled in approximately 15-ns increments.

To achieve reliable threshold detection of a single photoelectron, the signal from that photoelectron must be far enough above the noise such that false signals are sufficiently rare. For an acquisition system that includes an ADC, the single-photoelectron threshold should be set above a single least significant bit (LSB) of the converter. In general, this means that an N-bit converter provides $N–X$ bits of signal range, where X is selected to insure sufficiently low false-detection
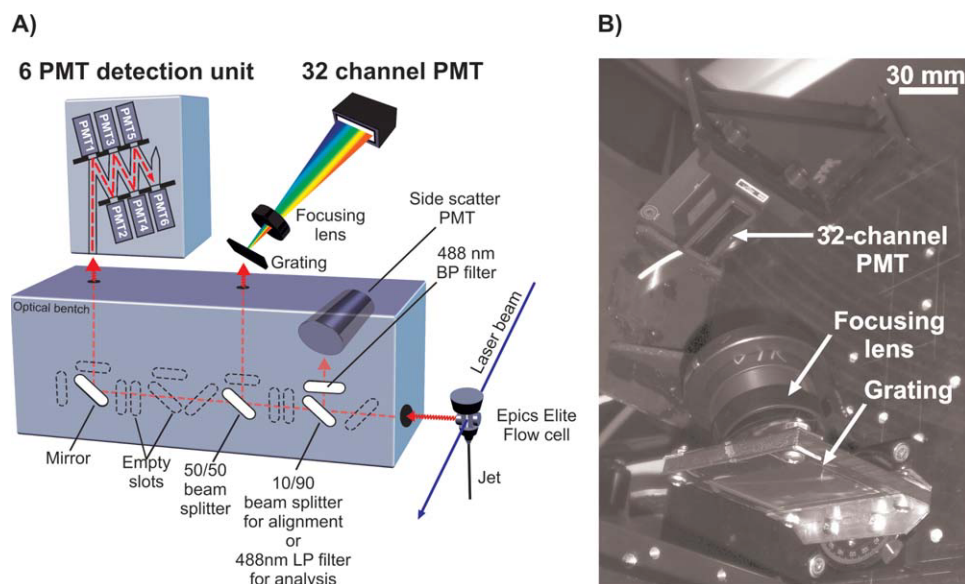
**Figure 1.** (**A**) Scheme of the commercial flow cytometer optical bench (Coulter Epics Elite) modified to detect side-scatter signal and fluorescence at the single-cell level using both a holographic grating positioned in front of a 32-channel multianode PMT and a 6-channel PMT-based polychrometer with the following set of bandpass filters: 525/30 nm (FITC) in front of PMT 1, 575/30 nm (PE) in front of PMT 2, 620/30 nm (PE—Texas Red) in front of PMT 3, 675/30 nm (PE-Cy5) in front of PMT 4, and 767/30 nm (PE-Cy7) in front of PMT 6. (**B**) Photograph of the optical system mounted on the Epics Elite cell sorter, with the phase-volume holographic grating and the 32-channel PMT. [Color figure can be viewed in the online issue, which is available at wileyonlinelibrary.com.]

probability for a single photoelectron. In the PhotoniQ-OEM Model 3214, X is ~2.5, which yields a 3,000-to-1 photoelectron dynamic range from its 14-bit converters. While this may seem considerably less impressive than the capabilities of current research-grade high-speed cytometers, it is not a significant problem for the described system since we are collecting the entire spectrum, and it is the complete spectral signature that we analyze, not selected individual spectral intensity bands. Consequently, the sensitivity at specific wavelengths, while important, is less crucial for a spectral subsystem, which evaluates the entire spectrum. There is a slight drop off in sensitivity toward the ends of the detector array, as shown in Figure 2A, but this can be largely overcome by incorporating digital processing (standardization) of each individual channel before output is analyzed.

The PhotoniQ-OEM Model 3214 board is specifically designed to interface to multianode PMTs, such as the Hamamatsu 7260-01 chosen for this project. Each of the 64 channels simultaneously integrates the output from a charge- or current-generating element of an array and performs analog-to-digital conversion. A digital signal processor (DSP) controls the data flow into its internal memory and allows for processing of the captured array data. Some processing functions are available as standard features (such as offset and gain adjustments for each channel). A maximum theoretical digitization rate of 75,000 complete 32-channel spectra per second at 14 bits is achievable for uniformly (in time) presented events. The PhotoniQ board allows fixed background currents to be dynamically canceled by the baseline restorer, and the system significantly reduces the baseline drift in conditions of large amplitude pulses at high repetition rates (pulse pile-up).

Additionally the board offers background subtraction. The system also provides various internal digital filtering options, but this functionality was not used in the reported work.

An internal DSP controls the flow of data from the parallel port of the PhotoniQ board to a digital IO card in the PC. Another reason for choosing the PhotoniQ-OEM Model 3214
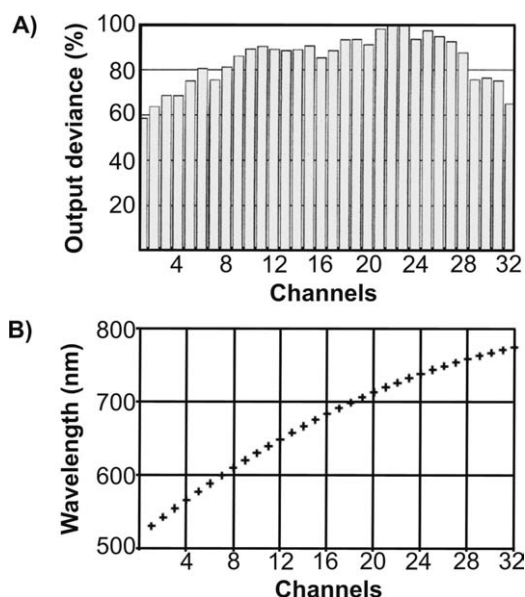
Figure 2. (**A**) Sensitivity of anodes in Hamamatsu 7260 PMT. (**B**) Correspondence between the 32 channels of the PMT and the wavelengths.

is that it has a standard connector interface designed for the PCI-6534 high-speed digital IO card from National Instruments. A LabView interface driver allows control of the card features from a PC through a serial port. However, owing to the limitations of LabView, a complete data-collection package was written in-house to operate the detection unit.

Forty-four simultaneous variables were recorded for each single particle analyzed on our cytometer. These consisted of 32 narrow bands of fluorescence from the multianode PMT (creating a spectral signature); 6 wide fluorescence bands from a parallel traditional 6-channel detector (FWHM30nm Type; Asahi Spectra U.S.A.); a side-scatter signal collected on a regular PMT; and 5 forward-scatter signals (4 angles + their sum) collected using an enhanced multiangle scatter-detection system. The detailed description of the latter can be found in Rajwa et al., 2008 (24).

Flow Cytometer

The FCM fluidics used for the presented spectral detection prototype was based on a customized EPICS Elite cell sorter (Beckman Coulter, Miami, FL). The system was equipped with two air-cooled lasers: (a) 488-nm JDS Uniphase 2211 Series argon laser system, 20 mW, and (b) a 633-nm JDS Uniphase 1135 HeNe laser, 10 mW, both of which were fiber coupled. A flow-cell tip with an orifice 100 μm in diameter was used on the instrument. Each round input beam is focused to an elliptical spot using crossed-cylindrical lenses of different focal lengths, each of which focuses the beam in only one dimension. The elliptical focal spots are estimated to be 5–12 μm high and ˜100 μm wide, similar to those of other conventional instruments (1).

The liquid sheath was distilled water filtered through a 0.2 μm pore–size filter. The pressure applied to the sheath tank was kept constant at 12 psi (82 kPa). A differential pressure of at least 0.5 psi was maintained between sample and sheath pressures to push the sample into the flow cytometer and avoid any contamination from backflush of the sheath fluid. The lymphocyte concentrations in the various samples analyzed were in the range of 1,000–3,500/μl. The sample pressure differential was adjusted to maintain a flow rate of ~1,000 events per second, although the maximum event rate we were able to run was about 3,000 events per second. With such a setup the jet velocity (V_{jet}) is 12.88 m/s, as can be calculated from the following equation (25): $V_{jet} = (2P/\rho)^{1/2}$ where P is the pressure (12 psi = 8.27.10^4 N/m^2) and ρ is the density of water at 20°C (0.998 kg/m^3).

As lymphocytes vary in size from 6 μm (slightly smaller than an RBC) up to 15 μm, their time of flight (TOF) is very short (< 2.10 μs), as displayed in Table 1.

In parallel to the 32-channel spectral unit, a traditional 6-channel detection system was installed on the cytometer in place of the original PMTs, to collect fluorescence signals in a manner identical to that of a traditional commercial 6-color FCM instrument (Fig. 1A). The 6-channel detection unit was based on a 30-nm FWHM polychromator from Asahi Spectra USA (Torrance, CA). This polychromator was equipped with 6 PMTs and the following set of bandpass filters: 525/30 nm

Table 1. Time of flight calculated for theoretical lymphocytes of 6 and 15 μm in diameter flowing at 12.88 m/s through a 5- or 12-μm laser focal spot

LASER HEIGHT (μm)	CELL DIAMETER (μm)	TOF (μs)
5	6	0.85
	15	1.55
12	6	1.40
	15	2.10

(FITC), 575/30 nm (PE), 620/30 nm (PE–Texas Red), 675/30 nm (PE-Cy5), and 767/30 nm (PE-Cy7). To split the fluorescent signal coming from the measured particles to perform simultaneous measurement using two units, a 50/50 beam splitter was placed between the 32-channel spectral subsystem and the 6-channel device.

To perform the alignment of the instrument at 90° a 10/90 beam splitter was used to send the 488-nm particle scatter to a regular PMT installed on the Elite to collect the right-angle light scatter. For the analysis, this beam splitter was changed to a 488-nm long pass filter. A 488-nm bandpass filter was placed in front of the PMT to collect only light scattered by the particles (cells) at 488 nm. The alignment was performed using Flow-Check^{TM} fluorescent microspheres (Beckman Coulter). Flow-Check^{TM} 770 fluorospheres from Beckman Coulter were also used to align the 32-channel PMT and the grating.

An enhanced multiangle forward-scatter detection system capable of measuring forward-scatter signals at four different angles was installed in place of a regular FS detector (26). However, for the purpose of this study only the sum of the signals detected at all four angles was used.

FCM Data Acquisition and Analysis Software

The acquisition and analysis of the 44-variable vector required development of a new, custom-built software package. The Cytospec program, a freeware that can be downloaded from http://www.cyto.purdue.edu/Purdue_software, is able to record and control all 44 values simultaneously for each single particle analyzed. Advanced statistical processing was also implemented in the package to process spectral information. With so many acquired variables traditional FCM data presentation methods such as 1-D histograms or 2-D cytograms were incapable of providing useful data visualization. Therefore, several data-reduction tools were implemented to display and analyze data (including principal component analysis (PCA), conversion of data vectors into hyperspherical coordinates, etc.).

Monoclonal Antibodies

CD45/FITC, CD4/PE, CD8/ECD, and CD3/Cy5 human monoclonal antibody tetra-color combination from mouse (catalog number 6607013) was obtained from Beckman Coulter (Miami, FL). CD19/PE-Cy7–labeled human antibody raised in mouse (catalog number 25-0199) was obtained from eBioscience (San Diego, CA).
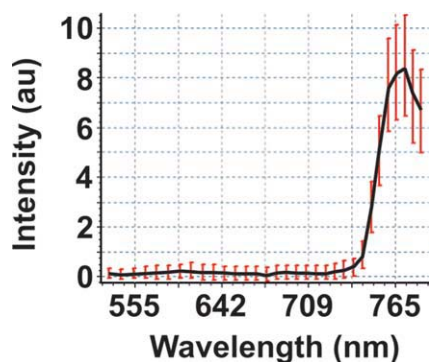
Figure 3. Average spectrum obtained from the analysis of 7,000 Flow Check^{TM} 770 fluorospheres by the 32-channel PMT. The bars represent the standard deviation of the data recorded for each of the 32 channels.

Blood Collection and Sample Preparation

Venous blood was collected under human-use protocol 0506002740 by a standard venipuncture procedure using 7-ml EDTA Venoject tubes. For all studies, a standard 100 μl whole blood was taken from the venous sample, mixed with 10 μl antibody solution, and incubated for 10 minutes at room temperature. All samples were prepped on a standard Q-prep using the 35-second cycle and the ImmunoPrep reagent system from Beckman Coulter.

RESULTS

Optical alignment of the 488-nm and 633-nm laser beams, the flow cell, and the photodetectors installed on the customized Epics Elite (the regular side-scatter PMT, the multiangle scatter-detection system, and the 6-channel detector) was achieved with the regular targets (metal plates) provided by Beckman Coulter. Fine-tuning was performed by analyzing fluorescent microspheres (Flow-Check^{TM} microspheres) to obtain the smallest possible CVs (<3%) of the forward- and side-angle light-scatter intensities.

The grating and the 32-channel PMT were installed at 90° to the laser beam direction. Half the point-source signal coming from the interrogation volume was directed to the grating by a 50/50 beam splitter. The final positions of the grating and the 32-channel PMT module were found when the signal was projected onto the 32-channel PMT (Fig. 1B). The alignment of the 32-channel PMT and grating was first performed by reflecting the collinear 488-nm and 633-nm beams at 90° onto the grating. The two wavelengths were then separated by the grating and the 32-channel PMT was placed in such a way that the 488-nm signal was recorded on the first and second channels. The red signal from the HeNe laser was displayed farther to the right on the 32-channel PMT. Even though the laser beams are monochromatic they were dispersed over more than one channel, likely because of the optics encountered by the beam (for instance, the focalization lens of the Epics Elite and the beam splitters mentioned above).

With gross alignment completed, the fine-tuning and the determination of the relative distribution of the wavelengths over the 32-channel PMT were accomplished by acquiring and analyzing signals from fluorescent microsphere solutions and biological control samples (i.e., stained with one fluorochrome only). The fine-tuning of the grating position allowed shifting the light collection toward longer wavelengths to avoid direct collection of the 488-nm photons scattered at 90°. Figure 3 presents results after the analysis of Flow-Check^{TM} 770 microspheres from Beckman Coulter. These microspheres have a maximal excitation at 488 nm and a maximal emission at 770 nm (which was assigned to Channel 30).

Blood-sample controls were prepared for lymphocyte analysis according to the Material and Methods by incubating different antibodies labeled with various fluorochromes (CD45/FITC, CD4/PE, CD8/ECD, and CD3/Cy5). Each control sample, incubated with one labeled antibody only, was run on the flow cytometer until at least 7,000 lymphocytes were analyzed. The lymphocytes were first gated using the FS-SS cytogram (Fig. 4A) and their spectra were analyzed. Figure 4B presents the average spectrum of 7,000 lymphocytes with the corresponding standard deviation.

Based on these spectra and the emission spectrum of each dye (provided by the manufacturer) it was then possible to superimpose the maximal emission wavelength of each dye onto the channel where the maximal signal was recorded. By interpolation, it was then possible to estimate the correspondence between the remaining channels on the 32-channel PMT and the other wavelengths (Fig. 2B). A polynomial regression of degree two was a good approximation of the data
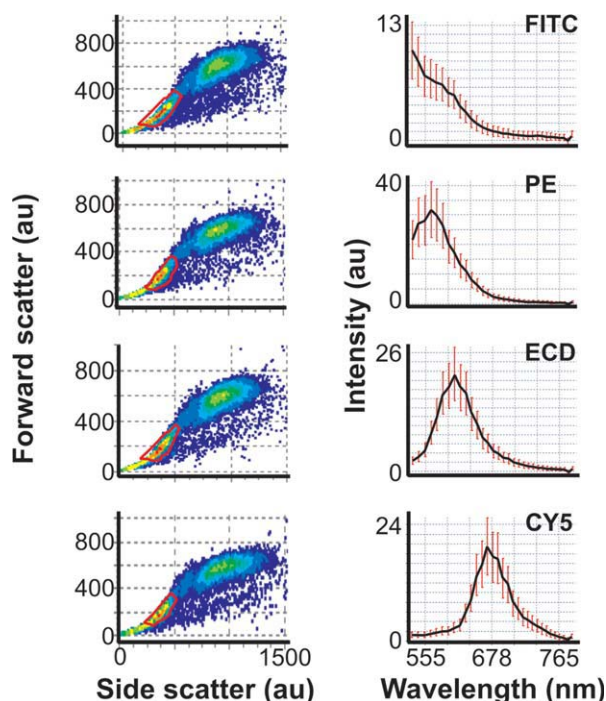
Figure 4. (**A**) Forward- versus side-scatter cytogram recorded for control samples consisting of blood labeled with a single antibody conjugated with either FITC, PE, ECD, or Cy5 (left column). These cytograms were used to gate out the lymphocytes from the rest of the particles (cells). (**B**) Corresponding average spectra (and standard deviation for each channel) obtained for each control from the spectra of 7,000 lymphocytes.
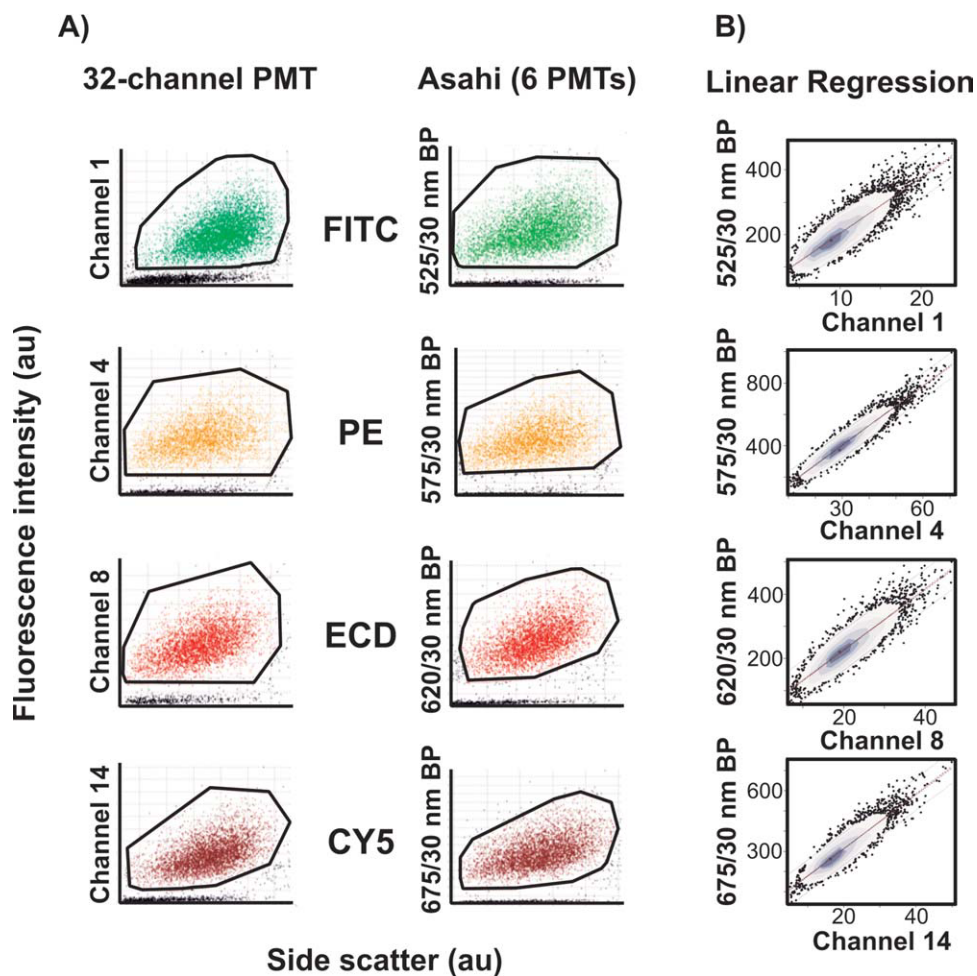
Figure 5. (**A**) Comparison between the signal collected by the 32-channel PMT (left column) and the Asahi device (right column) for each blood control sample. The cytograms displayed are side scatter versus the fluorescence intensity centered on the maximal emission of each dye for 7,000 events. (**B**) Comparison between the data provided by the 32-channel PMT (*X*-axis) and the Asahi device (*Y*-axis) for each blood control sample. For each plot, the gray area displays the high-density region of the data [light gray area contains 95% of the data centered on the mode]. Black dots are referred to as outliers. This representation shows that data are close to normality. The red line is the regression line. The dashed lines are the 95% confidence intervals of the regression. The dotted lines are the prediction intervals of the regression.

($R^2 = 0.997$) and allowed good estimation of all the channel values for which the wavelength was not measured. The following polynomial was used to generate Figure 2B: $y = -0.15x^2 + 12.998x + 517.81$, where x is the channel number and y the corresponding wavelength in nm.

One can see that the relationship is not linear: the red area of the spectrum is more spread out and the shorter wavelengths are more condensed. The result is a lower efficiency of signal collection in red, as can be illustrated by the low intensity recorded for the red fluorescent Flow-Check™ 770 microspheres (Fig. 4): the maximal intensity of only 8.5 au from these beads is recorded on channel 30 (corresponding to 769 nm). Therefore, it was not possible to collect signal from lymphocytes labeled with CD19/PE-Cy7. In addition, there is also a loss due to the mask located under the photocathode. This mask present between the channels does not permit signal collection. For this reason, in this report we use the term "estimate" to describe the correspondence between the 32 channels and the collected wave-lengths. Indeed, measuring the exact wavelength range collected by every channel was not feasible.

The spectral subsystem provides different information about analyzed particles than does a traditional wide-band system, which is mostly optimized for sensitivity and efficiency of photon collection. However, it was necessary to define a common denominator allowing us to visualize and compare data collected with both subsystems. Thus, datasets were simultaneously acquired by the Asahi 6-channel polychromator and the multiband PMT. Fluorescence versus SS cytograms were generated to display data collected either on the 6-channel Asahi polychromator or on the 32-channel spectral PMT for the exact same set of 7,000 lymphocytes (Fig. 5A):

• FITC signal collected on the Asahi PMT behind the 525/30 nm dichroic bandpass filter was compared with the corresponding signal collected on channel 1 of the 32-channel PMT.
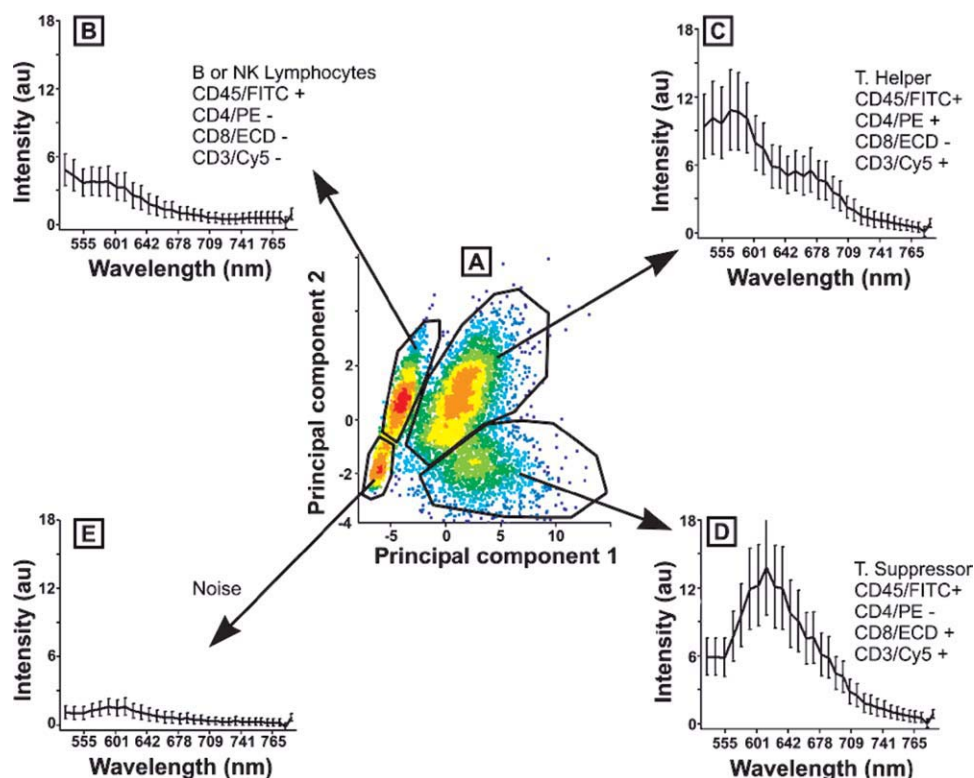
Figure 6. Result of the clustering performed by PCA on a blood sample incubated with antibodies labeled with four fluorochromes (FITC, PE, ECD, and Cy5) (**A**). Lymphocytes were first gated out from the rest of the particles on a forward-scatter versus side-scatter cytogram. In this example, four populations are discriminated based on the PCA. For each cluster, the average spectrum (and the standard deviation per channel) is displayed: B or NK lymphocytes (**B**), T helper lymphocytes (**C**), T suppressor lymphocytes (**D**), and noise/detritus (**E**).

- PE signal collected on the Asahi PMT behind the 575/30 nm dichroic bandpass filter was compared with the corresponding signal collected on channel 4 of the 32-channel PMT.
- ECD signal collected on the Asahi PMT behind the 620/30 nm dichroic bandpass filter was compared with the corresponding signal collected on channel 8 of the 32-channel PMT.
- PE-Cy5 signal collected on the Asahi PMT behind the 675/30 nm dichroic bandpass filter was compared with the corresponding signal collected on channel 14 of the 32-channel PMT.

Although the subsystems differ in terms of sensitivity and spectral resolution, both sets of data show highly correlated results as demonstrated by the linear regression in Figure 5B: the red lines are the regression lines; the dashed lines are the 95% confidence intervals of the regression; the dotted lines are the prediction intervals of the regression (27).

Following this validation step, a blood sample was incubated with all the antibodies. At least 7,000 lymphocytes were simultaneously analyzed by the spectral subsystem and the 6-channel Asahi device. Each lymphocyte was characterized by an emission spectrum that is a linear combination of the emission spectra of the dyes carried by the antibodies linked to it.

To achieve rapid classification of the various lymphocyte subsets based on their fluorescence signatures, PCA was performed on the fluorescence sub-vector by the Cytospec software (Fig. 6). The lymphocytes were first gated out from other cells (monocytes and granulocytes) and debris on the basis of the FS-SS cytogram; therefore these two variables were not included in the subsequent PCA. The data were not smoothed or normalized in any way prior to PCA. When the results are projected onto a new coordinate system defined by the first and second principal components, three clusters can readily be distinguished (Fig. 6A). For each one, delimited on the figure by a region, Cytospec provides the averaged spectrum with the standard deviation for every single channel. Based on the spectrum collected for each control sample it was then possible to identify the different subsets of lymphocytes:

- The B or NK lymphocytes, which were CD45/FITC$^+$, CD4/PE$^-$, CD8/ECD$^-$, and CD3/Cy5$^-$ (Fig. 6B) but which could not be distinguished because the signal from CD19/Cy7 was not recorded.
- The T helpers (Fig. 6C), which were CD45/FITC$^+$, CD4/PE$^+$, CD8/ECD$^-$, and CD3/Cy5$^+$.
- The T suppressors, which were CD45/FITC$^+$, CD4/PE$^-$, CD8/ECD$^+$, and CD3/Cy5$^+$ (Fig. 6D).

Since the lymphocytes were gated on the FS/SS cytogram, some other events (debris) might also have been included in the procedure. However, these events do not show any fluores-

cence compared to the lymphocytes (Fig. 6E) and can thus be easily discriminated and eliminated from the analysis.

DISCUSSION AND CONCLUSION

The majority of currently available FCM instruments operate in almost the same fashion as the systems built nearly 40 years ago. Biological particles (cells) flow in a single stream in the very center of the surrounding sheath fluid and are interrogated by excitation light (usually one or several laser beams). Light scattered by the particles or emitted owing to fluorescence is separated by a set of dichroic mirrors and filters and collected using photodetectors (1). A gradual move in design complexity from two to several colors steadily continued, and by 1997 published reports were describing the use of eight simultaneous fluorescence signals (28); by 2001 this number increased to 11 (6) and more recently to 18 colors (2). The goal remains to acquire more fluorescence signals simultaneously, which in practical terms means more functional information per analyzed cell. However, the principle of separating fluorescence by cascading dichroic mirrors and bandpass filters becomes unsustainable. Flow cytometers with 14 PMTs are typically equipped with a set of 30–40 optical filters for excitation blocking, spectral separation, and transmission of narrow bands. The number of filters becomes a serious issue as far as sensitivity is concerned, and the number of detectors is a problem in term of both price and compactness of the available instruments.

Currently available modern multianode photodetectors and fast collection boards equipped with DSP chips provide an alternative in FCM design. Instead of attempting to orthogonalize the fluorescence signals by the means of complex optics accompanied by compensation, to match every fluorochrome with a dedicated photodetector, one can use approaches known from chemometrics, remote sensing, or multispectral microscopy in which a few high-sensitivity wide-band detectors are accompanied by spectral subsystems. Issues such as low signal intensity owing to losses caused by dispersion, limited time for acquisition and analysis, and lack of easily available spectral-analysis programs that can work directly with flow cytometers have prevented the spectral technologies represented by multianode PMTs from moving into the mainstream. In this report, we have shown a feasibility study proving that a compact FCM system based on a multianode PMT can collect useful spectral information and can coexist with a modern but traditionally arranged 6-channel PMT module (20). Interestingly, the setup used for comparison raised the bar for the spectral subsystem in terms of collection efficiency. However, efficient detection and analysis of lymphocytes was possible, despite the fact that the spectral data were recorded with a 50/50 mirror present in the optical pathway. For other applications one can imagine a sequential data collection procedure in which a portion of the sample is characterized using a spectral subsystem and another portion of the sample is analyzed with the traditional detectors. Although the presented prototype was not highly optimized and the number of fluorophores relatively limited (four), it demonstrated sufficient sensitivity to collect fluorescence emission from biological particles and allowed discrimination of specific subsets of lymphocytes as defined by the four labeled antibodies. We also showed that use of a modern off-the-shelf rapid signal-collection board paired with appropriate software enables simultaneous registration of 44 variables in real time.

The single-PMT spectral approach has some attractive features. It simplifies the optical pathway significantly. However, the use of 32 bands does not necessarily add to data-analysis complexity and does not require that compensation (spectral unmixing) be performed for a simple exploratory analysis and visualization. By grouping cells into subpopulations directly by using their 32-channel spectral patterns as inputs for dimensionality reduction (via PCA), we were able to preview the populations without compensation, as demonstrated with the four fluorophores used in this work. For the purpose of the presented study the data analysis and subsequent clustering followed variable reduction using PCA; however, in principle, other data-reduction and/or classification techniques can be employed, such as kernelized PCA, independent component analysis, or convex cone analysis. If quantitative determination of label abundance is required a multispectral system can still use a linear spectral unmixing similar to traditional compensation, although the inversion of spectral matrix will be replaced by pseudo-inversion since the number of bands would exceed the number of labels (4,29). Additionally, other methods employed in spectral analysis such as neural networks or support vector machine—based classification may be considered (30).

Direct comparison of the spectral detection subsystem with the traditional detector module reveals a number of important differences:

- A single spectral PMT has the ability to collect more than double the number of bands collected by the most sophisticated polychromatic instruments available (22); since the sensitivity of a spectral system is lower, the increased number of bands does not directly imply an ability to resolve larger number of fluorochromes in a practical setting. However, like multispectral microscopy, the spectral subsystem will provide higher spectral resolution if intense signals are available, allowing for easy discrimination of highly overlapping labels.
- The footprint of the optics is considerably smaller and the optical pathways are much simpler, with a vastly reduced number of components. While initial versions of our multispectral cytometer had restricted wavelength sensitivity (maximum of 650 nm) (23), more recent versions of the Hamamatsu multianode PMTs have advanced this to 880 nm, more than adequate to handle all the currently used fluorescence probes; for the H7260-20 model the quantum efficiency is still satisfactory (50%) at 800 nm but drops to 2% only at 880 nm.
- The grating is not as efficient as high-quality dichroic mirrors, but improving the optical train more than compensates for this deficiency. However, alternative dispersion techniques involving prisms, may offer better efficiency and should be tested as well. The purpose of this article is to prove the feasibility of the method, and the reader must keep in mind that the whole setup is a prototype. There is

no doubt that a more careful design would improve the efficiency of the system.

- Since the 32 anodes in the currently used multianode PMT cannot be individually controlled, and the typical anode uniformity declared by the producer is 1:1.7 (1:2.5 maximum), it is necessary to standardize the output by performing gain compensation processing on all spectral data collected. The anode uniformity information with output deviations is provided by the PMT manufacturer, and can be verified by implementing a calibration procedure. It is likely that the new-generation multianode PMTs may offer individual fine control of every anode, allowing for even more flexible operation.

Clearly, handling and processing spectral data appears complex. However, there are a number of advantages in performing spectral analysis even for applications requiring traditional polychromatic systems. While raw signal intensity is indeed very important in FCM, it may be far less significant than the availability of complete spectral signatures. The reason is that individual fluorochromes are no longer represented by readout from a single detector, but rather by a pattern spread on multiple anodes. Consequently the ability to discriminate fluorochromes is limited by multivariate rather than univariate differences between subpopulations. This opens up new opportunities for supervised classification in which the analysis algorithms would be trained to recognize subpopulations based on their complete spectral patterns, rather than by using a binary positive (high intensity) versus negative (low intensity) distinction. Data-processing automation of full patterns (i.e., functional data) measured by FCM at the single-cell level has indeed proved to be an efficient tool for objective analysis and clustering of cells (31).

However, the new spectral approaches cannot be viewed as a panacea for the problem of multiplexing in FCM. The very design of the multianode PMTs limits their sensitivity and flexibility. If the detection of a minute amount of fluorescent label is the goal, there is still no better tool than a highly optimized and well-tuned traditional flow cytometer.

ACKNOWLEDGMENTS

LITERATURE CITED

1. Shapiro HM. Practical flow cytometry, 4th ed. Wiley: Hoboken; 2003. p 681.
2. Perfetto SP, Chattopadhyay PK, Roederer M. Seventeen-colour flow cytometry: Unravelling the immune system. Nat Rev Immunol 2004;4:648–655.
3. Sebba DS, Watson DA, Nolan JP. High throughput single nanoparticle spectroscopy. ACS Nano 2009;3:1477–1484.
4. Bagwell CB, Adams EG. Fluorescence spectral overlap compensation for any number of flow cytometry parameters. Ann N Y Acad Sci 1993;677:167–184.
5. Roederer M. Spectral compensation for flow cytometry: Visualization artifacts, limitations, and caveats. Cytometry 2001;45:194–205.
6. De Rosa SC, Herzenberg LA, Herzenberg LA, Roederer M. 11-color, 13-parameter flow cytometry: identification of human naive T cells by phenotype, function, and T-cell receptor diversity. Nat Med 2001;7:245–248.
7. Buican TN, Habbersett RC, Martin JC, Naivar MA, Parson JD, Wilder ME, Jett JH. DiDAC: A new FCM data acquisition and sorting system. Cytometry 1991;12:136.
8. Wade CG, Rhyne RH Jr., Woodruff WH, Bloch DP, Bartholomew JC. Spectra of cells in flow cytometry using a vidicon detector. J Histochem Cytochem 1979;27:1049–1052.
9. Steen HB. Simultaneous separate detection of low angle and large angle light scattering in an arc lamp-based flow cytometer. Cytometry 1986;7:445–449.
10. Stokke T, Steen HB. Fluorescence spectra of Hoechst 33258 bound to chromatin. Biochim Biophys Acta 1986;868:17–23.
11. Buican TN. Real-time Fourier transform spectroscopy for fluorescence imaging and flow cytometry. Proc SPIE 1990;1205:126–133.
12. Gauci MR, Vesey G, Narai J, Veal D, Williams KL, Piper JA. Observation of single-cell fluorescence spectra in laser flow cytometry. Cytometry 1996;25:388–393.
13. Asbury CL, Esposito R, Farmer C, van den Engh G. Fluorescence spectra of DNA dyes measured in a flow cytometer. Cytometry 1996;24:234–242.
14. Johnson PE, Lund ML, Shorthill RW, Swanson JE, Kellogg JL. Real time biodetection of individual pathogenic microorganisms in food and water. Biomed Sci Instrum 2001;37:191–196.
15. Goddard G, Martin JC, Naivar M, Goodwin PM, Graves SW, Habbersett R, Nolan JP, Jett JH. Single particle high resolution spectral analysis flow cytometry. Cytometry Part A 2006;69A:842–851.
16. Watson DA, Brown LO, Gaskill DF, Naivar M, Graves SW, Doorn SK, Nolan JP. A flow cytometer for the measurement of Raman spectra. Cytometry Part A 2008;73A:119–128.
17. Brown LO, Doorn SK. Optimization of the preparation of glass-coated, dye-tagged metal nanoparticles as SERS substrates. Langmuir 2008;24:2178–2185.
18. Brown LO, Doorn SK. A controlled and reproducible pathway to dye-tagged, encapsulated silver nanoparticles as substrates for SERS multiplexing. Langmuir 2008;24:2277–2280.
19. Goddard G, Brown LO, Habbersett R, Brady CI, Martin JC, Graves SW, Freyer JP, Doorn SK. High-resolution spectral analysis of individual SERS-active nanoparticles in flow. J Am Chem Soc 2010;132:6081–6090.
20. Robinson JP, Rajwa B, Patsekin V, Grégori G, Jones J. Purdue Research Foundation (West Lafayette, IN), assignee. Multispectral detector and analysis system. USA Pat. 7280204; 2007.
21. Robinson JP, Patsekin V, Gregori G, Rajwa B, Jones J. Multispectral flow cytometry: Next generation tools for automated classification. Microsc Microanal 2005;11:2–3;4.
22. Robinson JP, Rajwa B, Grégori G, Jones J, Patsekin V. Multispectral cytometry of single bio-particles using a 32-channel detector. Proc SPIE 2005;5692:59–365.
23. Robinson JP. Multispectral cytometry: The next generation. Biophot Int 2004;11:36–40.
24. Rajwa B, Venkatapathi M, Ragheb K, Banada PP, Hirleman ED, Lary T, Robinson JP. Automated classification of bacterial particles in flow by multiangle scatter measurement and support vector machine classifier. Cytometry Part A 2008;73A:369–379.
25. Van den Engh G. High-speed cell sorting. In: Durack G, Robinson JP, editors. Emerging Tools for Single Cell Analysis. New York: Wiley-Liss; 2000. p 21–48.
26. Venkatapathi M, Rajwa B, Ragheb K, Banada PP, Lary T, Robinson JP, Hirleman ED. High speed classification of individual bacterial cells using a model-based light scatter system and multivariate statistics. Appl Opt 2008;47:678–686.
27. Hyndman RJ. Computing and graphing highest density regions. Am Stat 1996;50:120–126.
28. Roederer M, De Rosa S, Gerstein R, Anderson M, Bigos M, Stovel R, Nozaki T, Parks D, Herzenberg L, Herzenberg L. 8 color, 10-parameter flow cytometry to elucidate complex leukocyte heterogeneity. Cytometry 1997;29:328–339.
29. Keenan MR, Timlin JA, Van Benthem MH, Haaland DM. Algorithms for constrained linear unmixing with application to the hyperspectral analysis of fluorophore mixtures. Proc SPIE 2002;4816:193–202.
30. Brown M, Gunn SR, Lewis HG. Support vector machines for optimal classification and spectral unmixing. Ecol Modell 1999;120:167–179.
31. Malkassian A, Nerini D, van Dijk MA, Thyssen M, Mante C, Grégori G. Functional analysis and classification of phytoplankton based on data from an automated flow cytometer. Cytometry Part A 2011;79A:263–275.